REGULAR ARTICLE

blood advances

Bahcc1 is critical for the aberrant epigenetic program in a mouse model of *MLL-ENL*–mediated leukemia

Akihide Nakamura,[1,2] Masahiro Masuya,[2] Makoto Shinmei,[1] Isao Tawara,[2] Tetsuya Nosaka,[1] and Ryoichi Ono[1]

[1]Department of Microbiology and Molecular Genetics and [2]Department of Hematology and Oncology, Mie University Graduate School of Medicine, Tsu, Japan

Key Points

- Hematopoietic stem and progenitor cells have distinct differentiation stage-specific immortalization potentials that involve Bahcc1.
- Results suggest a novel *MLL-fusion-Bahcc1* axis in *MLL*-fusion–mediated leukemogenesis.

In leukemogenesis, genotoxic stress in hematopoietic stem and progenitor cells (HSPCs) drives individual context-dependent programs of malignant transformation. In light of the various differentiation stages of HSPCs based on a recently revised definition using CD150/CD48, our analyses showed that a subpopulation of long-term repopulating HSCs was most susceptible to *MLL-ENL*–mediated transformation. An analysis of the molecular mechanism identified *Bromo-adjacent homology domain and coiled-coil containing 1* (*Bahcc1*), which encodes a reader molecule of trimethylated histone H3 lysine 27 (H3K27me3), as a candidate gene involved in distinct susceptibility to leukemic transformation. Interestingly, *Bahcc1* was previously reported to be highly expressed in acute myeloid leukemia (AML) with an unfavorable prognosis, including some cases of *MLL*-rearranged AML. We found that MLL-ENL upregulated *Bahcc1* through binding to its promoter, and that Bahcc1 was involved in *MLL-ENL*–mediated immortalization at least partly through repression of H3K27me3-marked *Cdkn1c*. Analyses using bone marrow transplantation in mice showed that depletion of *Bahcc1* suppressed the leukemogenic activity of *MLL-ENL*. In a public database, high *BAHCC1* expression was found to be associated with a poor prognosis in pediatric AML, in which *BAHCC1* expression was significantly lower in *MLL-AF9*-AML than in other *MLL-fusion*-AML. These findings shed light on the distinct immortalization potential of HSPCs and suggest a novel *MLL-fusion-Bahcc1* axis, which may lead to development of molecular targeted therapy against *MLL-fusion*–mediated leukemia.

Introduction

Acute myeloid leukemia (AML) is a hematological malignancy arising from a subpopulation of leukemic stem cells.[1-4] Previous studies[5-8] have shown that oncogenic events may transform normal hematopoietic stem cells (HSCs) and progenitor cells into leukemic stem cells. Interestingly, we have shown[9] that conditional expression of *MLL-ENL* leads to leukemic transformation of $CD34^{-}$c-$Kit^{high}Sca\text{-}1^{high}$-$Lineage^{-}$ (KSL) cells (previously defined as murine long-term repopulating HSCs [LT-HSCs]), but not that of $CD34^{+}$KSL cells (previously defined as murine short-term repopulating HSCs [ST-HSCs]) or myeloid progenitor cells. Recent advances[10-13] have also led to revision of the definition of HSCs and immature progenitor cells (HSPCs), using markers including CD150/CD48. However, little is known about the molecular mechanism of leukemic transformation in the "revised" HSPCs.

Submitted 27 July 2023; accepted 6 March 2024; prepublished online on *Blood Advances* First Edition 7 March 2024. https://doi.org/10.1182/bloodadvances.2023011320.

Next-generation sequencing data were deposited to the National Center for Biotechnology Information Gene Expression Omnibus under accession number GSE229484.

The full-text version of this article contains a data supplement.

A class of epigenetic regulators[14-18] has been found to play a key role in leukemogenesis. One epigenetic regulatory mechanism is suppression of expression of genes marked with trimethylated histone H3 lysine 27 (H3K27me3),[19-22] which is recognized by reader molecules, leading to chromatin compaction. In addition to the canonical readers, Bromo-adjacent homology (BAH) domain and coiled-coil containing 1 (BAHCC1), a large protein of 2608 amino acids, recognizes H3K27me3 via the BAH domain,[23,24] which is shared with BAH domain containing 1 (BAHD1). Both molecules mediate gene silencing by recruiting transcriptional repressor complexes. Interestingly, *BAHCC1* is highly expressed in AML with an unfavorable prognosis, including some cases of *MLL*-rearranged leukemia.[25] In addition, *BAHCC1* depletion suppresses growth of human leukemia cell lines expressing *MLL-AF4* in vitro, while *BAHCC1*/*Bahcc1* is critical for several types of leukemogenesis in vitro and in vivo but not for *BCR-ABL*–mediated leukemogenesis.[23] Thus, the precise role of *BAHCC1*/*Bahcc1* in *MLL*-fusion–mediated leukemogenesis remains unclear.

To investigate the molecular mechanism of *MLL*-fusion–mediated leukemogenesis in HSPCs more closely, we first examined the immortalization potential of *MLL-ENL* in "revised" HSPCs. The analyses showed that conditionally expressed *MLL-ENL* definitively immortalized "revised" LT-HSCs but did not have this effect on more differentiated multiple potent progenitor (MPP) cells and did not always immortalize immature progenitor cells. Comprehensive gene expression analyses of the HSPCs revealed increased expression of *Bahcc1* in the immortalized cells. In vitro analyses of the role of *Bahcc1* in leukemogenesis showed that MLL-ENL upregulated *Bahcc1* through promoter binding, and that Bahcc1 was involved in *MLL-ENL*–mediated immortalization, at least partly through repression of H3K27me3-marked *cyclin-dependent kinase inhibitor 1c* (*Cdkn1c*). Furthermore, in vivo analyses showed that depletion of *Bahcc1* suppressed the leukemogenic activity of *MLL-ENL*, suggesting that Bahcc1 may be a target for treatment of *MLL*-rearranged AML. Collectively, this study reveals distinct differentiation stage-specific immortalization potentials in HSPCs and describes a novel *MLL-fusion-Bahcc1* axis in *MLL*-fusion–mediated leukemogenesis.

Methods

Construct

pMYs retroviral vectors harboring a FLAG (DYKDDDDK peptide)-tagged *MLL-ENL* internal ribosomal entry site (IRES)-*neo*^{r} or -*EGFP* have been described elsewhere.[9] A 5'-fragment of *Bahcc1* generated with polymerase chain reaction (PCR) products using complementary DNA (cDNA) derived from immortalized LT-HSCs (described below) was combined with a fragment derived from a mouse cDNA clone M5C1031K16 (Dnaform, Tokyo, Japan) to produce full-length *Bahcc1* with a 3XFLAG tag at the C-terminus in pcDNA3.1 (Thermo Fisher Scientific Inc, Waltham, MA).

Mice

Compound C57BL/6 (B6) mice conditionally expressing *cytomegalovirus early enhancer/chicken β actin* (*CAG*) promoter–driven *MLL-ENL* by inducible Cre-estrogen receptor α chain (CreER) fusion protein expressed from the *Rosa26* locus (C/Tg mice) have been previously described.[9,26] All animal studies were approved by the Animal Care Committee of Mie University (no. 24-34-re5).

Purification of HSPCs

LT-HSCs (CD150$^+$/CD48$^-$KSL), ST-HSCs (CD150$^-$/CD48$^-$KSL), MPP2 (CD150$^+$/CD48$^+$KSL) cells, and MPP3/4 (CD150$^-$/CD48$^+$KSL) cells of C/Tg mice, and KSL and c-Kit^{high}Sca-1$^-$Lin$^-$ (hereafter designated MP) cells of wild-type B6 mice were purified from the respective bone marrow (BM) cells using a fluorescence-activated cell sorting (FACS) Aria II (BD Biosciences, Franklin Lakes, NJ).[9,26] In brief, lineage-depleted cells were isolated from BM mononuclear cells labeled with Lineage Cell Detection Cocktail-Biotin using a MACS cell separation system (Miltenyi Biotec, Auburn, CA). For purification of LT-HSCs, ST-HSCs, MPP2 cells, and MPP3/4 cells derived from C/Tg mice, lineage-depleted cells were stained with peridinin chlorophyll protein (PerCP)-Cy5.5-conjugated streptavidin, and phycoerythrin (PE)–conjugated anti-c-Kit (2B8), PE-Cy7–conjugated anti-Sca-1 (D7), allophycocyanin (APC)–conjugated anti-CD150 (TC15-12FL12.2), and brilliant violet 421 (BV421)–conjugated anti-CD48 (HM48-1) monoclonal antibodies. For purification of KSL and MP cells derived from wild-type B6 mice, lineage-depleted cells were stained with PerCP-Cy5.5–conjugated streptavidin, and PE-conjugated anti-Sca-1 (D7) and APC-conjugated anti-c-Kit (2B8) monoclonal antibodies. All monoclonal antibodies were purchased from BioLegend (San Diego, CA).

Retroviral transduction

Retroviral supernatants of Plat E cells transfected with a retroviral construct were harvested 48 hours after transfection.[27] Target cells were transduced with retroviruses using RetroNectin (TaKaRa Bio, Inc, Otsu, Japan).[28]

Myeloid immortalization assay

Myeloid immortalization assays via serial replating were performed as described elsewhere.[26] In brief, purified LT-HSCs, ST-HSCs, MPP2 cells, and MPP3/4 cells (150 cells) were directly sorted into 1.5 mL of methylcellulose medium prepared from M3234 (StemCell Technologies, Vancouver, Canada) according to the manufacturer's protocol, supplemented with 25 ng/mL mouse stem cell factor, 10 ng/mL each of human interleukin 6, mouse interleukin 3, and mouse granulocyte-macrophage colony–stimulating factor (Miltenyi Biotec), and 0.05 μM of 4-hydroxytamoxifen (Sigma-Aldrich, St Louis, MO) dissolved in ethanol or an equal amount of ethanol as a vehicle control. Sorted cells in 1 mL of the mixture were immediately plated in 35-mm dishes. KSL and MP cells retrovirally transduced with *MLL-ENL*-IRES-*neo*^{r} were also seeded in the same M3234-based methylcellulose medium supplemented with the same kinds of cytokines and 1 mg/mL G418 (Thermo Fisher Scientific Inc).

After culturing for 5 to 7 days, colonies were enumerated and single-cell suspensions (1×10^4 cells) of colonies were subsequently replated in α-MEM (Thermo Fisher Scientific Inc)–based medium containing 1% methylcellulose (Shin-Etsu Chemical Co, Ltd, Tokyo, Japan) supplemented with the same cytokines without 4-hydroxytamoxifen, ethanol, or G418. After the third round of plating, 5×10^3 of the cells forming >5 colonies were additionally replated. The colony-forming cells were harvested at the end of the fourth round of plating and were cultured in α-MEM supplemented

with 20% fetal bovine serum and the same cytokines to obtain immortalized cells that were capable of unlimited proliferation under liquid culture.

Gene silencing

The target sequences for *Bahcc1* and *luciferase* were 5′-GAAGAACCTGCTGAAATAC-3′ (shB-2) and 5′-AAAGTGGCCAACAAAGAGG-3′ (shB-8), and the shLuc sequence described elsewhere.[29] Short hairpin RNAs (shRNAs) sequences were inserted into pMXsU6-Kusabira Orange (KO)[9] or pMXsU6-puro (a kind gift from Toshio Kitamura, The Institute of Medical Science, University of Tokyo). Cells retrovirally transduced with pMXsU6-KO harboring an shRNA sequence were subjected to sorting according to expression of KO on the FACS Aria II 2-3 days after transduction. Cells transfected with pMXsU6-puro harboring an shRNA sequence were selected with 30 μg/mL puromycin (Sigma-Aldrich) for 48 hours at 2 days after transfection.

BMT

Assessment of leukemogenic activity in vivo was performed using BM transplantation (BMT).[9,30] Briefly, splenocytes were harvested from leukemic B6 mice in primary BMT using retrovirally *MLL-ENL*-IRES-*EGFP*–transduced KSL cells and were retrovirally transduced with shRNA/KO expressors in pMXsU6-KO. At 48 hours after transduction, 900 green fluorescent protein $(GFP)^+$ cells with high KO expression were sorted using the FACS Aria II and immediately transplanted into sublethally irradiated (5.25 Gy) recipient B6 mice. BM and spleen tissues from morbid mice were analyzed as described elsewhere.[30]

RNA seq and data analysis

Candidate genes involved in the differential modes of myeloid immortalization among HSPCs were found on the basis of their increased expression levels (log2 fold change [FC] >1 in induced ST-HSCs and log2 FC >0 in induced MPP2 cells, or log2 FC >1 in induced MPP2 cells and log2 FC >0 in induced ST-HSCs, with adjusted *P* values < .05) in RNA sequencing (RNA seq). Genes that were abundantly detected (count per million >10 in induced ST-HSCs and MPP2 cells and their respective controls) were focused on, followed by selection of genes with exclusive enhancement of expression in $CD34^-$ KSL cells, compared with that in $CD34^+$ KSL cells, in a previous cDNA microarray analysis.[9]

Statistical analysis

An unpaired Welch *t* test and 1-way analysis of variance followed by a Tukey-Kramer or Dunnett test as a post hoc test were used to compare 2 groups and >2 groups, respectively. Quantitative PCR (qPCR) data were log2-transformed before statistical analysis. The probability of overall survival of the mice, and that of patients with AML from public databases, was estimated using the Kaplan-Meier method and compared using log-rank tests, with Bonferroni correction in comparison among 3 groups. All statistical tests were performed using GraphPad Prism 9 (GraphPad Software, San Diego, CA).

FACS, immunoprecipitation (IP), western blotting, RNA seq, reverse transcription/chromatin immunoprecipitation (ChIP)–qPCR, gene silencing in human leukemic cell lines, and bioinformatics analysis are described in the supplemental Methods.

All animal studies were approved by the Animal Care Committees of Mie University (No. 24-34-re5)

Results

LT-HSCs are immortalized by conditional expression of *MLL-ENL*, but MPP3/4 cells are not, whereas ST-HSCs and MPP2 cells are not always immortalized

To examine the immortalization potential of *MLL-ENL* in the "revised" HSPCs, LT-HSCs, ST-HSCs, MPP2 cells, and MPP3/4 cells from C/Tg mice were subjected to myeloid immortalization assays by conditional expression of *MLL-ENL* (Figure 1A-B; supplemental Figure 1). Although nearly equal expression levels of *MLL-ENL* were induced at the end of the initial plating (Figure 1C), only LT-HSCs definitely formed compact colonies composed of morphologically myelomonocytic blasts (Figure 1D) after serial replating, whereas MPP3/4 cells did not do so. ST-HSCs and MPP2 cells formed colonies in 5 of 7 trials after serial replating (Figure 1B). In addition, in transferring cells harvested from the fourth plating into liquid culture for generating immortalized cells, the cells harvested from LT-HSC-derived replatable colonies always proliferated under liquid culture, whereas those harvested from ST-HSC- or MPP2-derived replatable colonies did so in only 2 of 7 trials (Figure 1B-C).

We next examined the expression levels of critical genes regulated by *MLL*-fusion genes in myeloid immortalization (Figure 1E). Initially, *Hoxa9* and *Evi1*, and *Hoxa9* alone, were significantly upregulated in LT-HSCs, and MPP2 cells, respectively. *Meis1* was also upregulated but did not reach statistical difference. After serial replating, expression levels were significantly elevated in the respective colony-forming cells derived from LT-HSCs, ST-HSCs, and MPP2 cells, except for that of *Meis1* in ST-HSC-derived cells. Interestingly, in contrast to immortalized ST-HSCs, immortalized LT-HSCs and MPP2 cells exhibited similar immunophenotypes of surface antigens, such as Gr-1/CD11b, but no differences in apoptotic subpopulations were found among these 3 types of immortalized cells (Figure 1F). These findings suggest that LT-HSCs were most susceptible to *MLL-ENL*–mediated transformation.

Conditional expression of *MLL-ENL* enhances expression of *Bahcc1* in LT-HSCs, but not in ST-HSCs or MPP2 cells, during myeloid immortalization

To examine the molecular mechanism involved in the differences in immortalization potential among HSPCs, we searched for differentially expressed genes among the induced LT-HSCs, ST-HSCs, MPP2 cells, and MPP3/4 cells at the end of initial plating in myeloid immortalization assays. At first, RNA extracted from induced ST-HSCs and MPP2 cells (at the end of initial plating) that would later be found to acquire colony-forming ability after the fourth round of plating were compared with the corresponding EtOH–treated control cells. RNA seq analysis of ST-HSCs and MPP2 cells revealed several differentially expressed genes (Figure 2A-B). Among these genes, expression of *Bahcc1* (more enhanced) and *Pik3r6* was exclusively enhanced in $CD34^-$ KSL cells in comparison to $CD34^+$ KSL cells, in a reanalysis of our previous cDNA microarray results[9] using conditional expression of *MLL-ENL* by retroviral transduction of *CreER* (Figure 2C; supplemental Table 1).

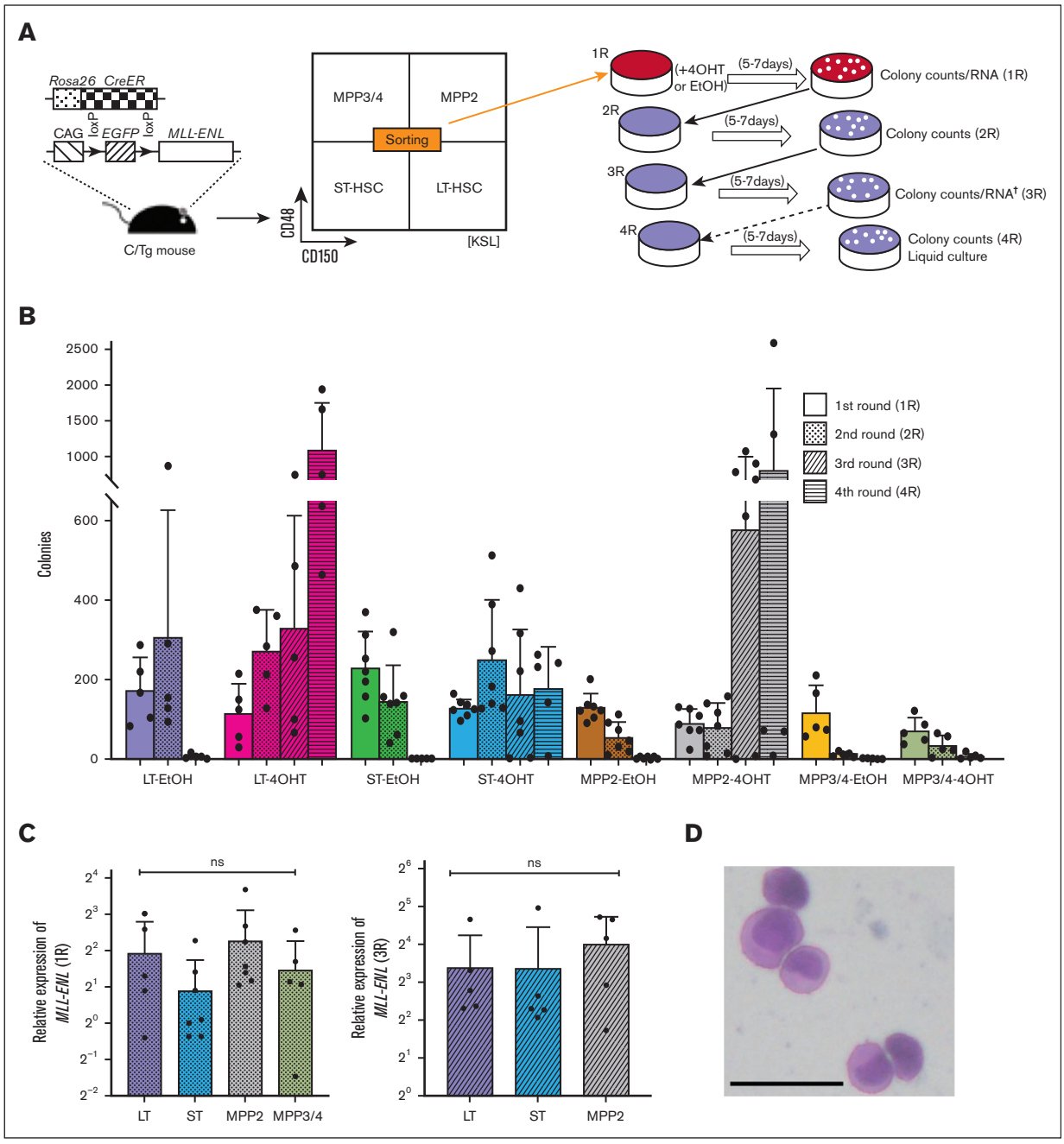

Figure 1. Myeloid immortalization potential of LT-HSCs, ST-HSCs, MPP2 cells, and MPP3/4 cells with conditional expression of *MLL-ENL*. (A) Experimental strategy for myeloid immortalization assays using serial replating. LT-HSCs, ST-HSCs, MPP2 cells, and MPP3/4 cells were purified from BM cells derived from C/Tg mice conditionally expressing *CAG* promoter-driven *MLL-ENL* by inducible Cre-estrogen receptor α chain (CreER) fusion protein expressed from the *Rosa26* locus by sorting with CD150/CD48 expression in KSL-gated cells. Initially, 100 cells from sorted cells were seeded with 4-hydroxytamoxifen (4OHT) or EtOH, followed by serial replating of 10^4 cells without drug. In cases with >5 colonies at the end of the third round (3R) of plating, 5×10^3 cells were replated for 4R plating. †RNA was extracted only from initially 4OHT-treated cells. (B) Myeloid immortalization assays. (C) Reverse transcription (RT)-qPCR of *MLL-ENL* in colony-forming cells at the end of initial plating (1R) and third plating (3R) in myeloid immortalization assays. (D) Typical morphology of immortalized LT-HSCs constituting the colonies. Cells with Wright-Giemsa staining were viewed with an Olympus CKX41 microscope using a ×4/0.13 objective lens, and an Olympus BX41 microscope using a ×20/0.5 objective lens. Images were acquired with Olympus DP21 software. Original magnification, ×200; bar, 50 μm. (E) RT-qPCR of *Hoxa9*, *Meis1*, and *Evi1* in colony-forming cells at the end of initial plating (with treatment of EtOH or 4OHT) and third plating (only cells derived from initially 4OHT-treated LT-HSCs, ST-HSCs, and MPP2 cells) in myeloid immortalization assays. In several samples from MPP3/4 cells, expression levels of *Evi1* were below the limit of detection. Colors and patterns of bars are the same as shown in panel B. (F) Representative FACS plots of immortalized LT-HSCs, ST-HSCs, and MPP2 cells. Bar graphs show the mean with standard deviation (SD) of at least 3 independent experiments. $^*P < .05$; $^{**}P < .01$; $^{***}P < .001$; $^{****}P < .0001$; ns, not significant (analysis of variance [ANOVA] followed by Tukey-Kramer multiple comparisons for panels C and E and unpaired Welch *t* tests for panel E).

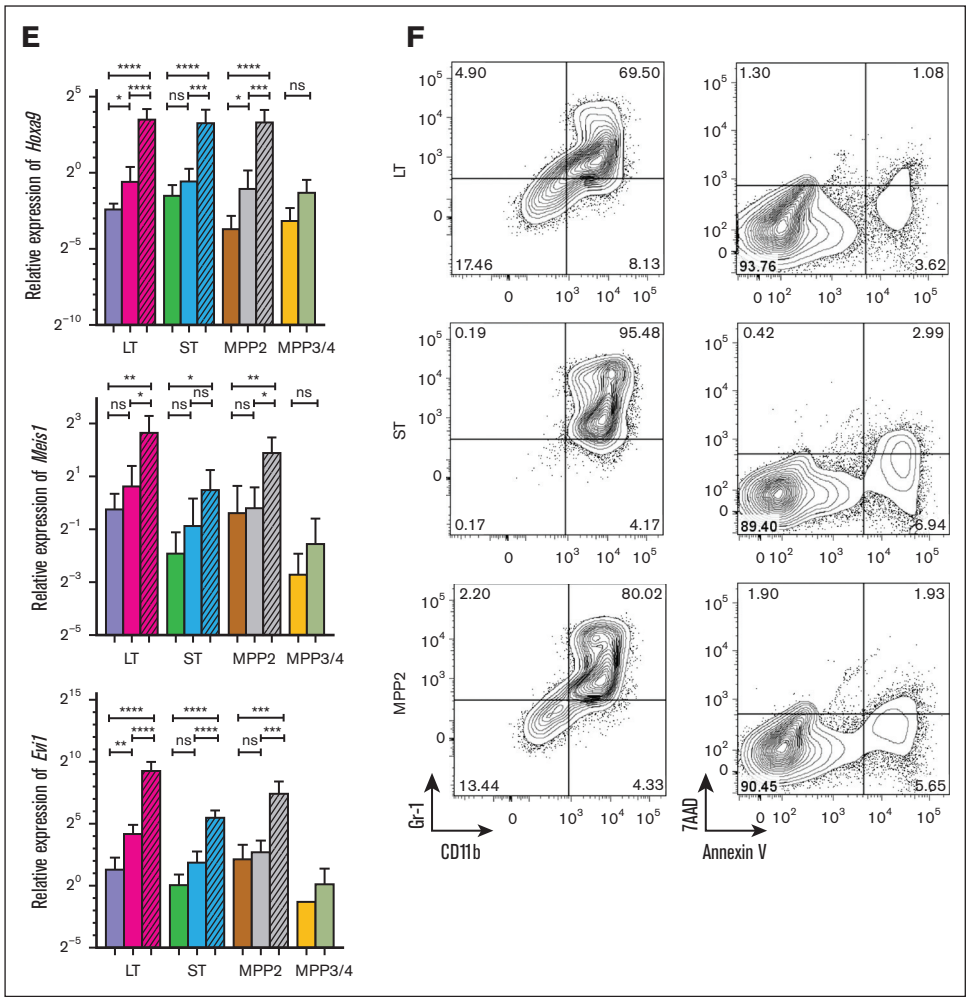

Figure 1 (continued)

Since LT-HSCs and MPP3/4 cells were enriched for CD34$^-$ and CD34$^+$ KSL cells, respectively, in C/Tg mice (Figure 2D), we examined expression of *Bahcc1* in induced HSPCs. Unexpectedly, *Bahcc1* expression at the initial plating was unchanged in the induced cells compared with corresponding controls and did not differ among induced HSPCs. However, *Bahcc1* expression at the third plating was significantly increased in induced LT-HSCs, ST-HSCs, and MPP2 cells. Significant enhancement (compared with that at initial plating) was only found in induced LT-HSCs (Figure 2E). These results suggest that *MLL-ENL* immortalized LT-HSCs with enhanced expression of *Bahcc1* but did not always immortalize ST-HSCs or MPP2 cells, despite moderate (but not significant) enhancement of *Bahcc1* expression.

Bahcc1 is critical for *MLL-ENL*–mediated immortalization of LT-HSCs

Next, to examine the involvement of *Bahcc1* in myeloid immortalization of LT-HSCs by *MLL-ENL*, *Bahcc1* was retrovirally depleted in immortalized LT-HSCs using shRNAs (shB-2 and shB-8) that could deplete Bahcc1 in 293 cells stably expressing Bahcc1 (Figure 3A-C). The *Bahcc1*-depleted cells exhibited a significant reduction in clonogenicity, and the reduction was more marked in shB-2–transduced cells than in shB-8 transduced cells (Figure 3D). In addition, we found a significant increase in the apoptotic subpopulation as well as a significant reduction in the Gr-1$^-$/c-kit$^+$ subpopulation with high potential for colony replating[31] in colony-forming cells derived from shB-2-transduced cells (Figure 3E). In colony-forming cells derived from shB-8-transduced cells, we found a tendency toward a reduction in the Gr-1$^-$/c-kit$^+$ subpopulation, but no increase in the apoptotic subpopulation. In contrast, there were no significant changes in the Gr-1$^+$/CD11b$^+$ subpopulation with myeloid differentiation, or in *Hoxa9*, *Meis1*, and *Evi1* expression (Figure 3F). These results suggest that MLL-ENL conferred aberrant self-renewal and anti-apoptotic activities on LT-HSCs, at least in part through Bahcc1, without affecting myeloid differentiation.

MLL-ENL upregulates *Bahcc1* via promoter binding

High expression of *BAHCC1* has been found in some AML cases with an unfavorable prognosis,[25] but little is understood about the molecular mechanism of upregulation of *BAHCC1*. Because a recent study[32] showed that *Mll*-deficiency reduces *Bahcc1* expression and that Mll binds just upstream of *Bahcc1* exon 2 in intestinal stem cells, we examined whether MLL-ENL upregulates

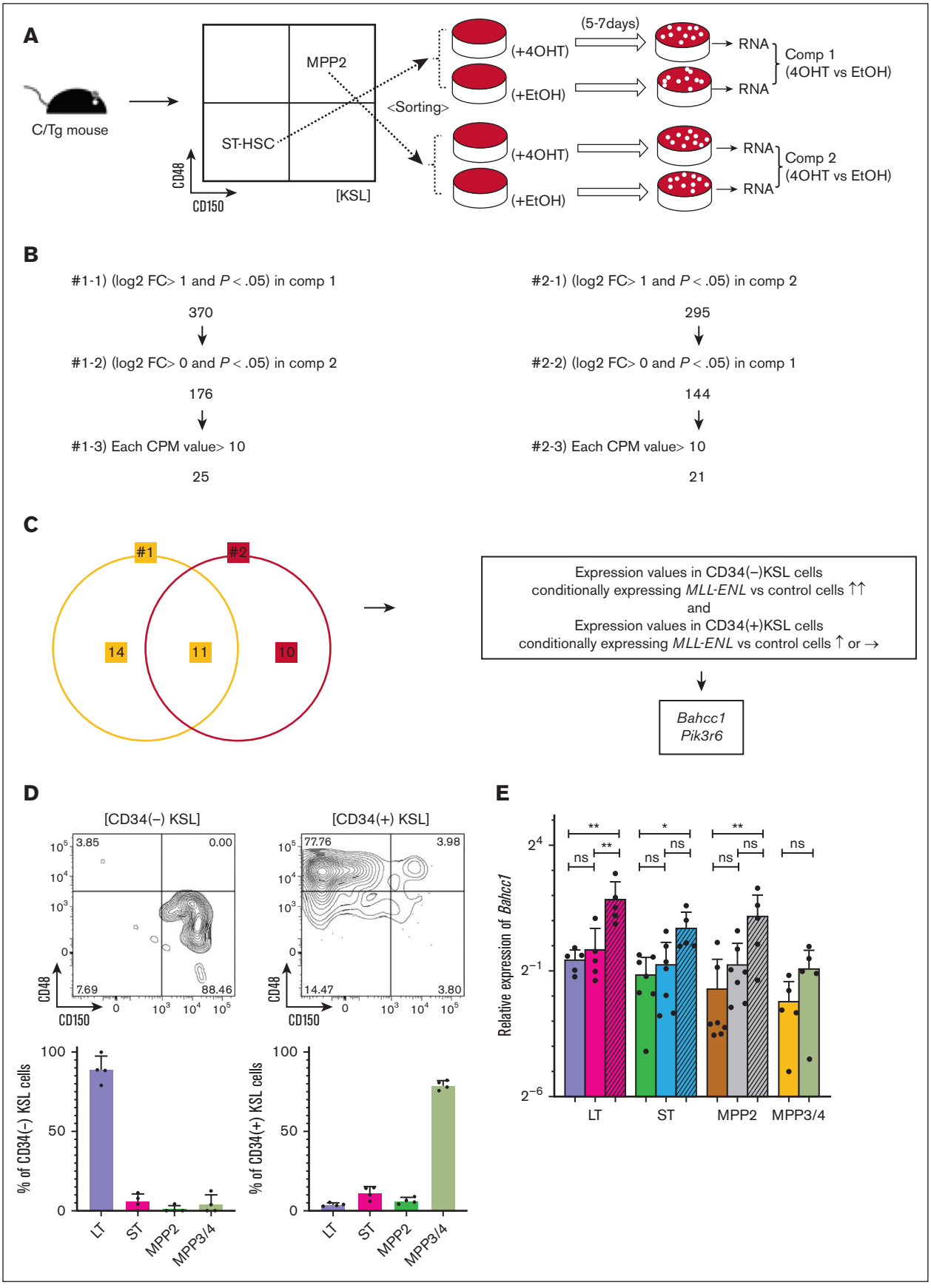
A
C/Tg mouse
MPP2
ST-HSC
CD48
CD150
[KSL]
<Sorting>
(+4OHT)
(+EtOH)
(5-7days)
RNA
Comp 1
(4OHT vs EtOH)
Comp 2
(4OHT vs EtOH)
B
#1-1) (log2 FC> 1 and P < .05) in comp 1
370
#1-2) (log2 FC> 0 and P < .05) in comp 2
176
#1-3) Each CPM value> 10
25
#2-1) (log2 FC> 1 and P < .05) in comp 2
295
#2-2) (log2 FC> 0 and P < .05) in comp 1
144
#2-3) Each CPM value> 10
21
C
#1
#2
14
11
10
Expression values in CD34(–)KSL cells
conditionally expressing MLL-ENL vs control cells ↑↑
and
Expression values in CD34(+)KSL cells
conditionally expressing MLL-ENL vs control cells ↑ or →
Bahcc1
Pik3r6
D
[CD34(–) KSL]
[CD34(+) KSL]
3.85
0.00
7.69
88.46
77.76
3.98
14.47
3.80
% of CD34(–) KSL cells
% of CD34(+) KSL cells
LT
ST
MPP2
MPP3/4
E
Relative expression of Bahcc1
ns
**
*

Figure 2.

Bahcc1 via promoter binding. In myeloid immortalization assays using wild-type KSL and MP cells retrovirally transduced with FLAG-tagged-*MLL-ENL*, expression of *Bahcc1* was significantly increased at the initial and third plating, and was also significantly more enhanced at the third plating in *MLL-ENL*-transduced-KSL cells (Figure 4A), similar to the enhancement in induced LT-HSCs. ChIP-qPCR assays of immortalized KSL cells showed a significant increase in MLL-ENL binding to regions around the putative transcription start sites of *Bahcc1*, as found in public ChIP-seq data showing enrichment of trimethylated histone H3 lysine 4 and RNA polymerase II in thymus, BM, and small intestine cells (Figure 4B-C). In addition, public ChIP-seq data (DRA004871[33] and GSE79899[34]) in several human *MLL*-rearranged leukemic cell lines, including HB1119 cells expressing *MLL-ENL*, also exhibited enrichment of MLL fusion proteins around the corresponding regions of human *BAHCC1*, accompanied with transcriptionally active histone marks and RNA polymerase II (supplemental Figure 2). Therefore, these results suggest that MLL-ENL upregulated *Bahcc1* via promoter binding during immortalization of HSPCs.

Bahcc1 is involved in *MLL-ENL*–mediated immortalization, at least partly through repression of H3K27me3-marked *Cdkn1c*

To examine the role of Bahcc1 in myeloid immortalization of HSPCs by *MLL-ENL*, we focused on several genes, including *Cdkn1c*, *Cdkn2a*, and *Cdkn2b*, which were found to be epigenetically regulated by Bahcc1.[23] Considering the results of our *Bahcc1* knockdown experiments, the expression levels of *Cdkn1c*, *Cdkn2a*, and *Cdkn2b*, which are involved in regulation of the cell cycle and apoptosis, were analyzed in immortalized LT-HSCs with *Bahcc1* depletion. For analysis in the early phase after *Bahcc1* depletion, shRNA-transduced cells were sorted and directly analyzed at 72 hours after transduction because it was difficult to analyze cells that were cultured for 24 hours after sorting at the regular time (48 hours after transduction). Although the condition of less efficient depletion of *Bahcc1* should be noted, expression of *Cdkn1c* tended to be increased in shB-2–transduced cells, but not in shB-8-transduced cells, whereas expression of *Cdkn2a* and *Cdkn2b* was not changed in either group of cells (Figure 5A).

In line with the results obtained in the early phase, expression of *Cdkn1c* was significantly increased in colony-forming cells derived from shB-2–transduced cells but not in cells derived from shB-8 transduced cells, whereas expression of *Cdkn2a* and *Cdkn2b* was not changed in either group of cells (Figure 5B). Interestingly, *Bahcc1* depletion was abrogated in the colony-forming cells, indicating that cells escaping from *Bahcc1* knockdown were dominant during culture after sorting. In addition, to examine whether *Cdkn1c* was epigenetically regulated by Bahcc1 by binding to H3K27me3 in *MLL-ENL*-immortalized HSPCs, ChIP-qPCR assays of immortalized KSL cells were performed around previously described regions.[35] These assays showed a significant increase in H3K27me3 around the tested regions of *Cdkn1c* (Figure 5C). Thus, these results suggest that depletion of Bahcc1 led to derepression of *Cdkn1c* through reduction of its binding to H3K27me3 marks in the regulatory genomic regions of *Cdkn1c* in *MLL-ENL*-immortalized cells.

Bahcc1 is also critical for *MLL*-fusion–mediated leukemogenesis of HSPCs in vivo

Finally, to further examine the role of *Bahcc1* in the molecular mechanism of *MLL-ENL*-mediated leukemogenesis in vivo, we analyzed the leukemogenic activity of *Bahcc1*-depleted leukemic cells using a secondary BMT model (Figure 6A). Primary *MLL-ENL*-transduced leukemic cells were efficiently depleted with *Bahcc1* by shB-2 and were transplanted into recipient mice (Figure 6B). In secondary BMT within an observation period of ~100 days, 6 of 12 recipient mice who underwent transplantation with *Bahcc1*-depleted leukemic cells died, whereas 10 of 10 control mice died (Figure 6C). Both groups of moribund mice similarly exhibited splenomegaly (Figure 6D) and most of their BM cells were GFP/KO-positive myelomonocytic cells (Figure 6E), indicating development of secondary AML. However, in spite of expression of KO in most BM cells, expression of *Bahcc1* in the BM cells of the 2 groups did not differ (Figure 6F), indicating that leukemic cells escaping from depletion of *Bahcc1* were dominant during development and/or progression of secondary AML. Interestingly, in some of the recipient mice who underwent transplantation with *Bahcc1*-depleted cells, the fluorescence intensity of KO was lower than that in control mice (Figure 6E). Expression of KO in peripheral white blood cells and BM cells was not detected at 53 and 100 days after BMT, respectively, in surviving mice transplanted with *Bahcc1*-depleted cells.

Analyses of the link between *BAHCC1* and human AML in public databases revealed an association of high expression of *BAHCC1* with a poor prognosis in pediatric Therapeutically Applicable Research to Generate Effective Treatments (TARGET) AML cohorts, but not in the adult Cancer Genome Atlas AML project (TCGA LAML) cohort (supplemental Figure 3A-D). A similar association was found in *MLL*-rearranged AML (supplemental Figure 3E) and in nonrearranged AML (supplemental Figure 3F) in the recent TARGET AML cohort. Gene set enrichment analyses of *MLL*-rearranged AML cohorts (GSE17855[36] and GSE61804[37]) revealed that high expression of *BAHCC1* was most closely associated with a gene set upregulated by *MYC*[38] in C6 oncogenic signature gene sets (Figure 7A; supplemental Figure 4A). The enrichment in the gene set upregulated by *MYC* was also

Figure 2. Possible involvement of *Bahcc1* in myeloid immortalization by conditional expression of *MLL-ENL*. (A) Initial screening strategy of candidate genes involved in differential modes of myeloid immortalization using induced ST-HSCs and MPP2 cells by RNA seq. (B) Numbers of differential expression genes (DEGs) screened by RNA seq in comparisons 1 (log2 FC>1 in induced ST-HSCs and log2 FC >0 in induced MPP2 cells, with adjusted *P* values <.05) and 2 (log2 FC >1 in induced MPP2 cells and log2 FC >0 in induced ST-HSCs, with adjusted *P* values <.05). Genes abundantly detected (count per million [CPM] >10 in induced ST-HSCs and MPP2 cells, and their respective controls) were focused on. (C) Refinement of focused genes based on exclusive enhancement in CD34 (–) KSL cells conditionally expressing *MLL-ENL* in the previous study.[9] *Bahcc1* and *Pik3r6* were selected from the focused genes among DEGs. Overlap of the focused genes in comparisons 1 and 2 is also shown. (D) Representative FACS plots and quantification of HSPCs based on CD150/CD48 expression in CD34(–) and CD34(+) KSL cells. (E) RT-qPCR of *Bahcc1* in myeloid immortalization assays using the same samples as shown in Figure 1E. Colors and patterns of bars are the same as shown in Figure 1E. Bar graphs show the mean with SD of at least 3 independent experiments. $^{*}P < .05$; $^{**}P < .01$; ns, not significant (ANOVA followed by Tukey-Kramer multiple comparisons and unpaired Welch *t* test for panel E).

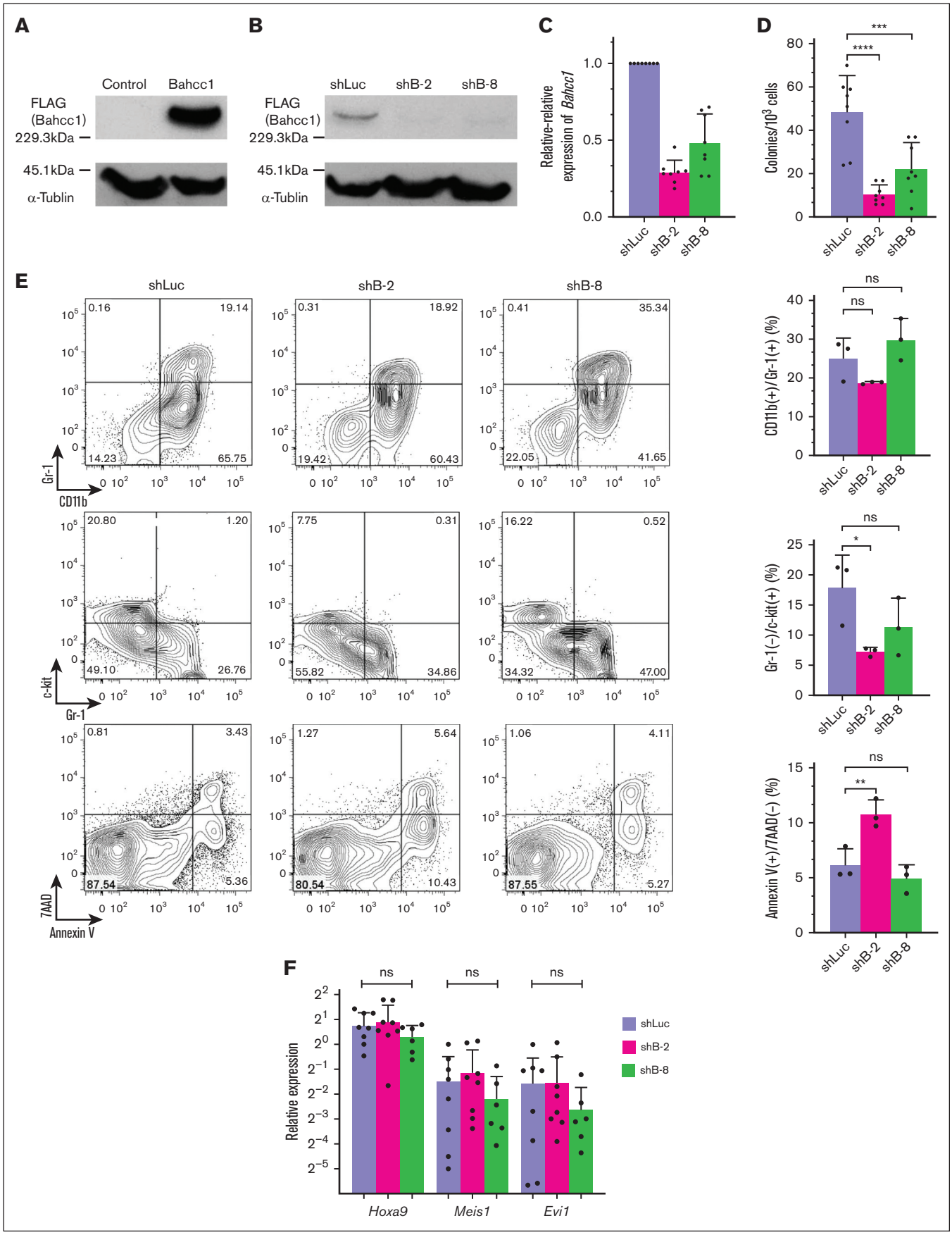
A
Control
Bahcc1
FLAG (Bahcc1) 229.3kDa
45.1kDa
α-Tublin
B
shLuc
shB-2
shB-8
FLAG (Bahcc1) 229.3kDa
45.1kDa
α-Tublin
C
Relative-relative expression of Bahcc1
shLuc
shB-2
shB-8
D
Colonies/10³ cells
E
shLuc
shB-2
shB-8
Gr-1
CD11b
c-kit
Gr-1
7AAD
Annexin V
CD11b(+)/Gr-1(+) (%)
Gr-1(−)/c-kit(+) (%)
Annexin V(+)/7AAD(−) (%)
F
Relative expression
Hoxa9
Meis1
Evi1
shLuc
shB-2
shB-8

Figure 3.

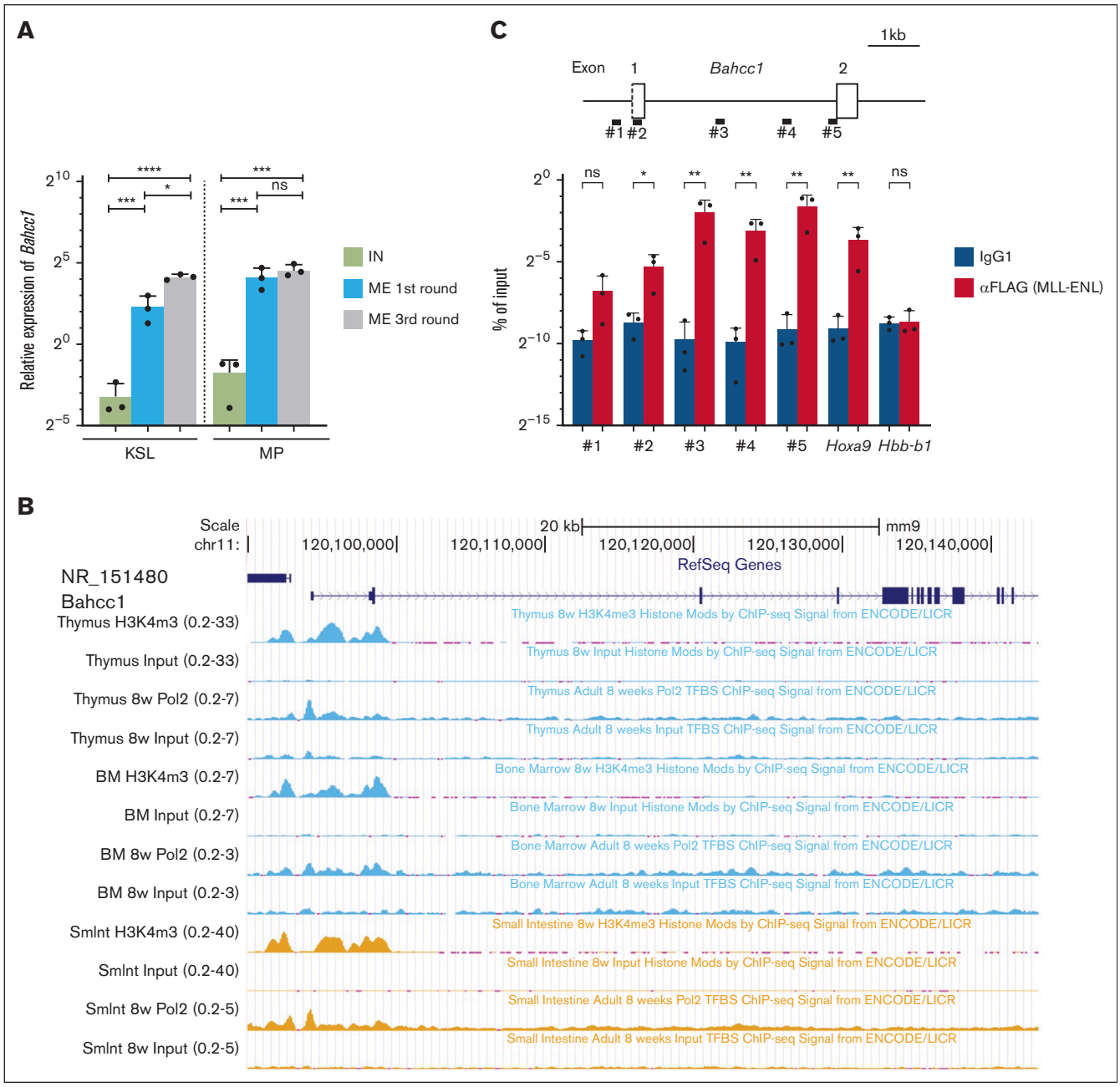

Figure 4. MLL-ENL upregulates *Bahcc1* via promoter binding. (A) RT-qPCR of *Bahcc1* in myeloid immortalization assays using wild-type *MLL-ENL*- (ME) or empty vector- (IN) transduced KSL and MP cells. (B) Overview of the genomic region of the *Bahcc1* locus in an adapted UCSC Genome Browser view. ChIP-seq data from mouse thymus, BM, and small intestine (SmInt) are shown in the LICR tracks (H3K4m3 and input control, Pol II, and input control). (C) ChIP-qPCR of MLL-ENL around exons 1 and 2 of *Bahcc1* using retrovirally FLAG-tagged-*MLL-ENL*-immortalized KSL cells. Primer sets (1-5) are shown (top). *Hoxa9* and *Hbb-b1* were used as controls. Bar graphs show the mean with SD of at least 3 independent experiments. $^{*}P < .05$; $^{**}P < .01$; $^{***}P < .001$; $^{****}P < .0001$; ns, not significant (ANOVA followed by Tukey-Kramer multiple comparisons for panel A and unpaired Welch *t* tests for panel C). IgG1, IgG subclass 1.

Figure 3. Bahcc1 depletion suppressed myeloid immortalization of LT-HSCs by conditional expression of *MLL-ENL*. (A-B) Western blot analyses of Bahcc1 in 293 cells (293^{Bahcc1}) that stably expressed 3XFLAG-tagged Bahcc1 (A), and in shRNA-transduced 293^{Bahcc1} cells (B). 293 cells transduced with pcDNA3.1 vector alone were used as a negative control in panel A. shRNAs against *luciferase* (shLuc, a negative control) and *Bahcc1* (shB-2 and shB-8) were transduced into 293^{Bahcc1} cells in panel B. Immunoprecipitants with anti-FLAG antibody were blotted with anti-DDDDK-tag antibody to detect expression of Bahcc1 (upper panels). α-Tubulin was analyzed in total lysates as an internal control (bottom panels). (C-D) Relative-relative expression levels of *Bahcc1* (C) in immortalized LT-HSCs with shRNA transduction and clonogenicity (D) of the cells. (E-F) Representative FACS plots and quantification of $CD11b^{+}$/Gr-1^{+}, Gr-1^{-}/c-kit^{+}, and apoptotic (annexin V^{+}/$7AAD^{-}$) subpopulations by FACS (E), and RT-qPCR of *Hoxa9*, *Meis1*, and *Evi1* (F) in colony-forming cells derived from immortalized LT-HSCs with depletion of *Bahcc1*. Bar graphs show the mean with SD of at least 3 independent experiments. $^{*}P < .05$; $^{**}P < .01$; $^{***}P < .001$; $^{****}P < .0001$; ns, not significant (ANOVA followed by Dunnett multiple comparisons for panels D-F).

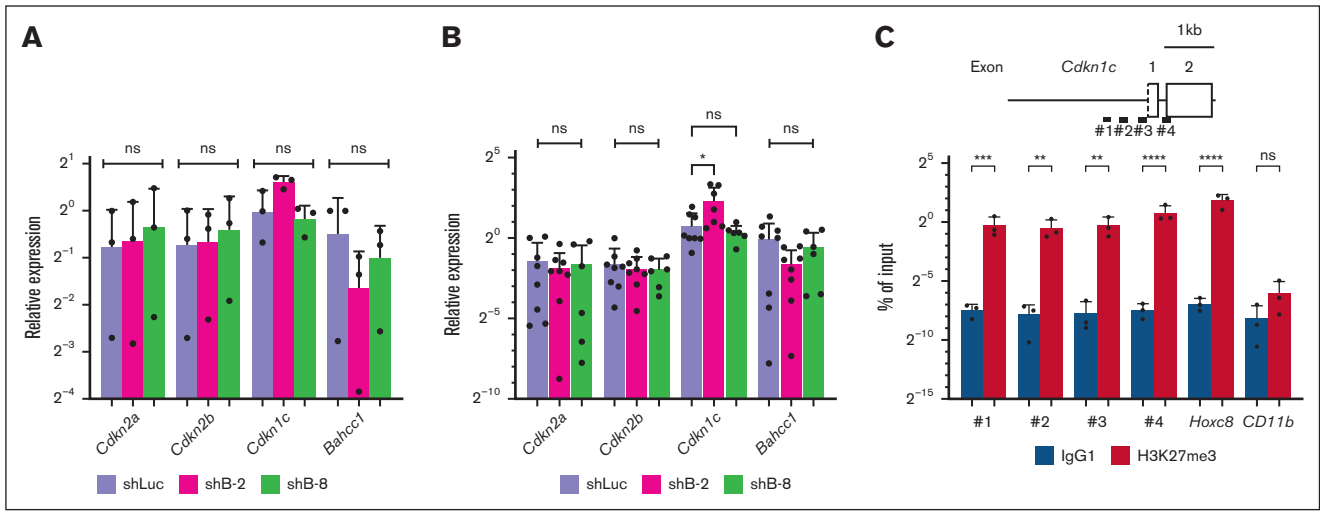

Figure 5. Derepression of *Cdkn1c* in immortalized LT-HSCs with *Bahcc1* depletion. (A-B) RT-qPCR of *Cdkn2a*, *Cdkn2b*, *Cdkn1c*, and *Bahcc1* in immortalized LT-HSCs transduced with shRNA/KO expressors. Cells sorted on the basis of high KO expression 72 hours after transduction (A), and colony-forming cells (B) derived from the shRNA-transduced cells shown in Figure 3C were analyzed. (C) ChIP-qPCR of H3K27me3 around exon 1 of *Cdkn1c* using FLAG-tagged-*MLL-ENL*-immortalized KSL cells. Primer sets (1-4) are shown (top). *Hoxc8* and *CD11b* were used as controls. shLuc, shRNA against *luciferase*; shB-2 and shB-8, different shRNAs against *Bahcc1*. Bar graphs show the mean with SD of at least 3 independent experiments. $^{*}P < .05$; $^{**}P < .01$; $^{***}P < .001$; $^{****}P < .0001$; ns, not significant. ANOVA followed by Dunnett multiple comparisons for panels A-B and unpaired Welch *t* tests for panel C.

found, although not significantly, in another AML data set (GSE19577[39]; supplemental Figure 4B). In line with this finding, expression of *Myc* tended to be reduced in colony-forming cells derived from immortalized LT-HSCs with *Bahcc1* depletion by shB-2 (Figure 7B). Interestingly, *BAHCC1* expression was significantly lower in AML with *MLL-AF9* than in AML with other *MLL*-fusion genes, in *MLL*-rearranged AML in childhood (GSE19577[39]; Figure 7B) and the recent TARGET AML cohort (supplemental Figure 4C). *BAHCC1* depletion suppressed cell proliferation in human leukemic cell lines, HB1119 cells expressing *MLL-ENL* and THP-1 cells expressing *MLL-AF9*, although derepression of *CDKN1C* was limited (supplemental Figure 5).

Taken together with the results for *MLL-ENL*-immortalized cells with *Bahcc-1* depletion in vitro, these in vivo results suggest that *Bahcc-1* depletion suppressed development and/or progression of *MLL-ENL*–mediated AML and that *BAHCC1* had an important role in *MLL*-fusion–mediated myeloid leukemogenesis, although a decrease in engraftment of depleted cells should be noted. Therefore, our results suggest that upregulation of *Bahcc1* by MLL-ENL is critical for *MLL-ENL*–mediated leukemogenesis, at least partly through epigenetic repression of expression of the negative cell-cycle regulator Cdkn1c.

Discussion

Here, we showed that $CD150^{+}/CD48^{-}$KSL cells (LT-HSCs) were the most susceptible targets for leukemic immortalization by *MLL-ENL* among HSPCs in our conditional transgenic mouse model. This finding is compatible with our previous results[9] showing that $CD34^{-}$KSL cells enriched for LT-HSCs are exclusively transformed by conditionally expressed *MLL-ENL*. However, this study also showed that the induced *MLL-ENL* could confer leukemic immortalization on ST-HSCs and MPP2 cells, albeit not in every experiment. These results imply that MPP cells might harbor fewer intrinsic advantages to *MLL-fusion*–mediated leukemogenesis than LT-HSCs. This is partly consistent with previous studies[7,40] showing more aggressive leukemogenesis by *MLL-AF9* or *MLL-ENL* in LT-HSCs, but not with another study[41] that showed intrinsic protection of LT-HSCs against *MLL-ENL*–mediated leukemogenesis. These differences might be explained by the differences in mouse models, including the promoters used and the mode of conditional or inducible expression[42,43]; however, further analyses are needed.

This study also revealed the role of the *MLL-ENL-Bahcc1* axis in leukemogenesis by *MLL-ENL*, at least partly through repression of H3K27me3-marked *Cdkn1c*.[44] This finding is reminiscent of a recent study[45] suggesting that the DNA methylation reader MBD2 developed *MLL-AF9*–driven leukemogenesis through repression of *Cdkn1c* transcription by binding to its methylated genomic promoter region. *BAHCC1* depletion suppressed the growth of human leukemic cell lines expressing *MLL-ENL* or *MLL-AF9*, but with limited derepression of *CDKN1C*. These findings suggest the possible involvement of BAHCC1-mediated repression of other tumor suppressor genes as well in *MLL*-fusion–mediated leukemogenesis, which needs further investigation. Interestingly, *Bahcc1* depletion did not change the expression of *Hoxa9*, *Meis1*, or *Evi1* in immortalized LT-HSCs, implying that Bahcc1 is an independent key player in *MLL-ENL*–mediated leukemogenesis. In addition, we found a close association of high expression of *BAHCC1* with a gene set upregulated by *MYC* by gene set enrichment analysis, and a tendency for reduction in expression of *Myc* in immortalized LT-HSCs with *Bahcc1* depletion. This finding does not agree with results showing no alterations in *MYC* expression in T-cell leukemic/lymphoma cell lines transduced with missense mutations abrogating BAH function by genome editing of *BAHCC1*.[23] These differences might imply possible functions of the BAHCC1/Bahcc1 region other than the BAH domain, which occupies only ~4.6% of the protein.

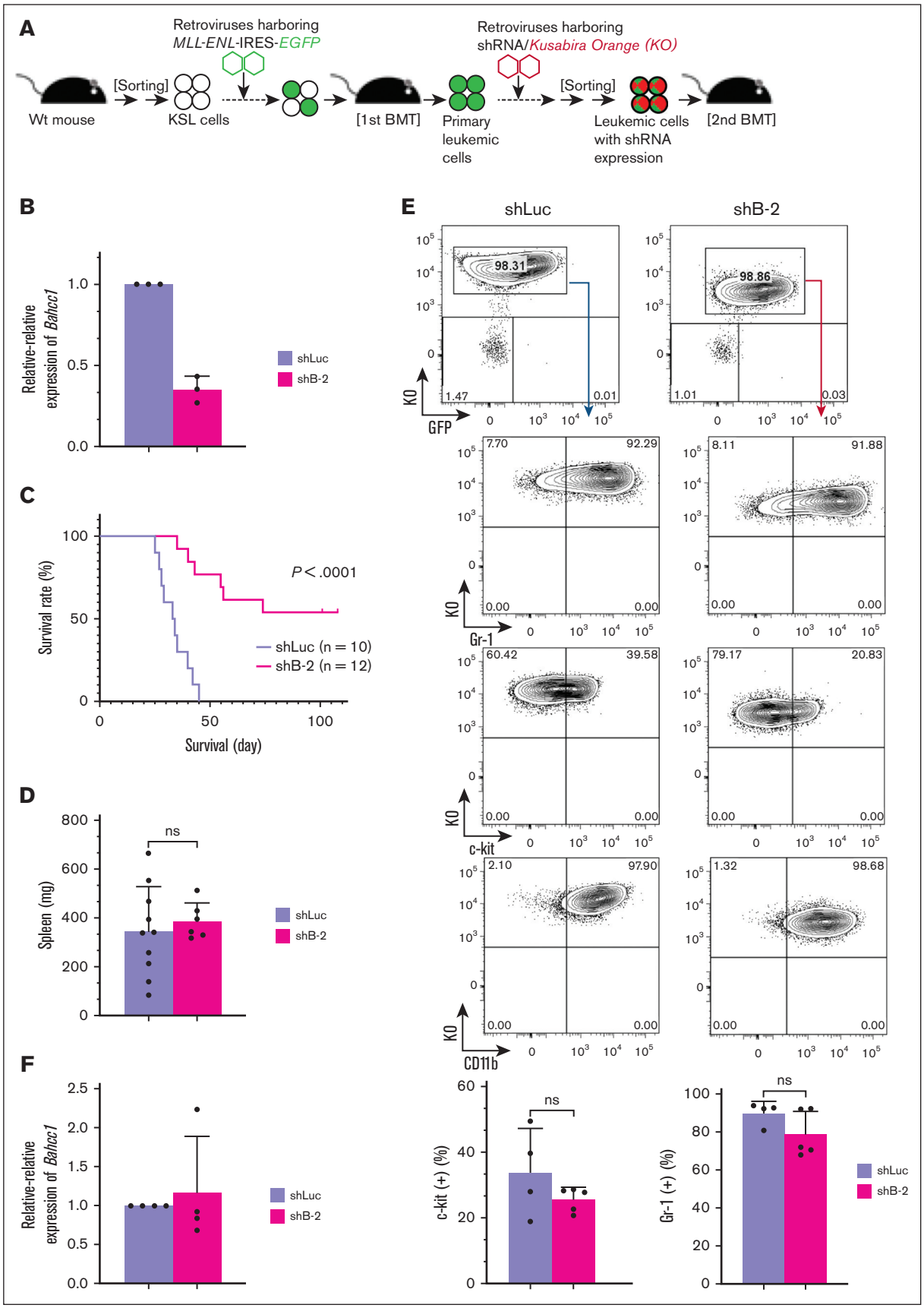
A
Retroviruses harboring
MLL-ENL-IRES-EGFP
Retroviruses harboring
shRNA/Kusabira Orange (KO)
[Sorting]
[Sorting]
Wt mouse
KSL cells
[1st BMT]
Primary leukemic cells
Leukemic cells with shRNA expression
[2nd BMT]
B
Relative-relative expression of Bahcc1
1.0
0.5
0.0
shLuc
shB-2
C
Survival rate (%)
100
50
0
P < .0001
shLuc (n = 10)
shB-2 (n = 12)
0
50
100
Survival (day)
D
Spleen (mg)
800
600
400
200
0
ns
shLuc
shB-2
F
Relative-relative expression of Bahcc1
2.5
2.0
1.5
1.0
0.5
0.0
shLuc
shB-2
E
shLuc
shB-2
98.31
98.86
1.47
0.01
1.01
0.03
KO
GFP
7.70
92.29
8.11
91.88
0.00
0.00
Gr-1
60.42
39.58
79.17
20.83
c-kit
2.10
97.90
1.32
98.68
CD11b
c-kit (+) (%)
60
40
20
0
ns
Gr-1 (+) (%)
100
80
60
40
20
0
ns
shLuc
shB-2

Figure 6.

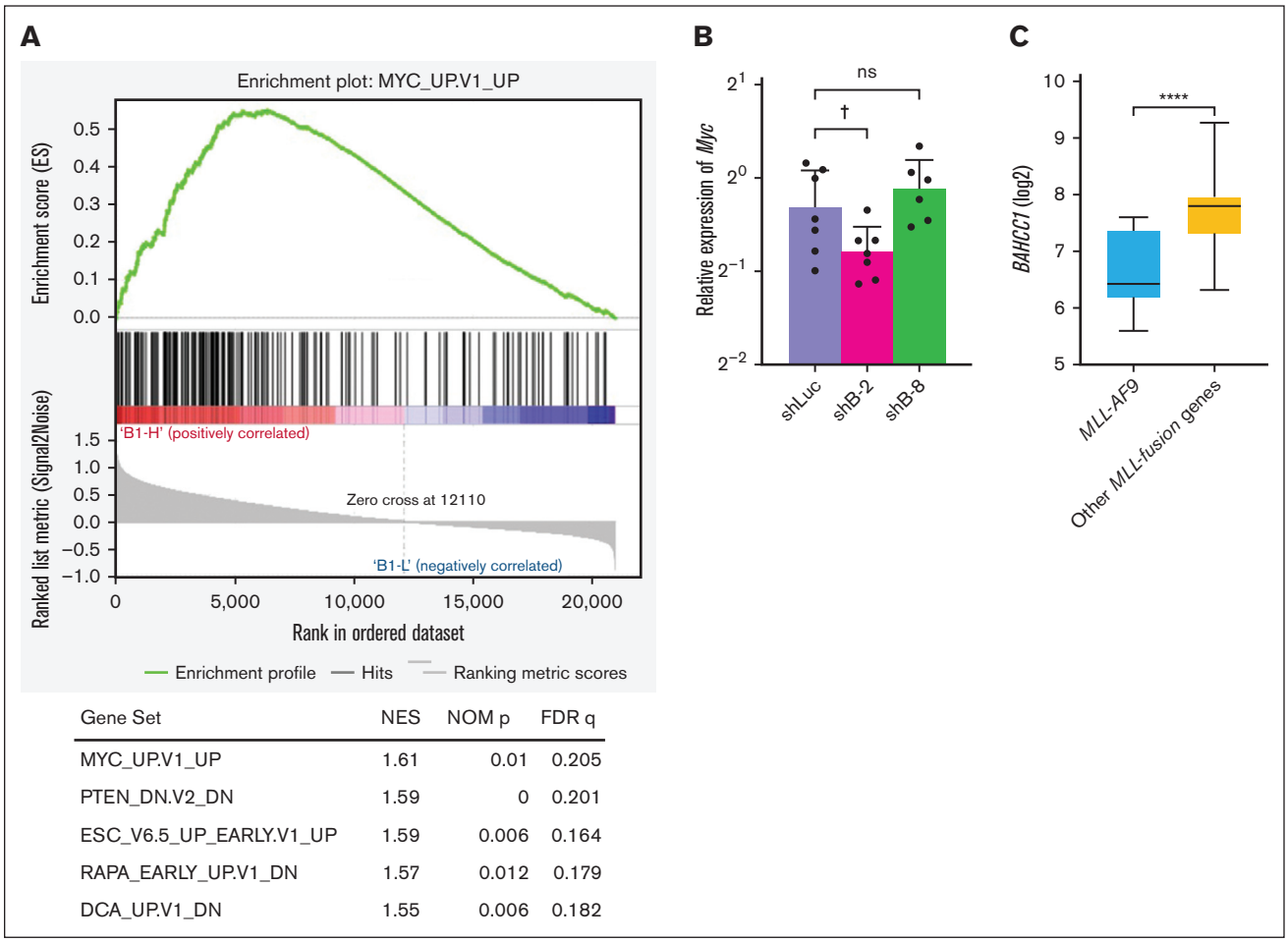

Gene Set	NES	NOM p	FDR q
MYC_UP.V1_UP	1.61	0.01	0.205
PTEN_DN.V2_DN	1.59	0	0.201
ESC_V6.5_UP_EARLY.V1_UP	1.59	0.006	0.164
RAPA_EARLY_UP.V1_DN	1.57	0.012	0.179
DCA_UP.V1_DN	1.55	0.006	0.182

Figure 7. *BAHCC1* is critical for *MLL*-rearranged AML. (A) Gene set enrichment analysis (GSEA) of *MLL*-rearranged AML samples (GSE17855[36]) with high (B1-H, n = 9) and low (B1-L, n = 9) expression of *BAHCC1* using C6 oncogenic signature gene sets. GSEA plot using the most enriched gene set, MYC_UP.V1_UP,[38] and a list of the top 5 enriched gene sets are shown (filtered by NOM (nominal) $P < .05$ and FDR $q < 0.25$). NES, normalized enrichment score. (B) RT-qPCR of *Myc* in colony-forming cells derived from the *Bahcc1*-depleted cells shown in Figure 3C. Bar graphs show the mean with SD of at least 3 independent experiments. (C) Expression levels of *BAHCC1* in AML samples (GSE19577[39]) with *MLL-AF9* (n = 11) and other *MLL*-fusion genes (n = 31). Data are shown in box and whisker plots. $^{\dagger}P = .054$; $^{****}P < .0001$; ns, not significant ANOVA followed by Dunnett multiple comparison for panel B and Mann-Whitney *U* test for panel C.

Our results in vivo showed prolonged latencies in BMT assays of *Bahcc1*-depleted leukemic cells, which is consistent with the association of high *BAHCC1* expression with aggressive *MLL*-rearranged AML in childhood, but careful interpretation is still required. Xenograft BMT assays with *BAHCC1* depletion also had prolonged latencies,[23] but all mice tested developed lethal disease, in contrast to our results. However, bioluminescent signals of *BAHCC1*-depleted cells in vivo were much weaker at the early time point after BMT, suggesting reduced homing and/or engraftment in BMT assays. The significantly lower expression of *BAHCC1* in *MLL-AF9*-AML might be involved, at least partly, in the relatively better prognosis in *MLL-AF9*-AML,[46] but further analysis, including elucidation of the mechanism of the *MLL-AF9*–associated lower expression, is required. Furthermore, the precise role of Bahcc1 in normal hematopoiesis should be addressed for development of novel therapies targeting the *MLL-fusion-BAHCC1* axis,

Figure 6. *Bahcc1* depletion prolongs development of *MLL-ENL*-induced leukemia. (A) Experimental strategy using secondary BMT. Primary leukemic cells expressing *MLL-ENL* together with *EGFP* were harvested, followed by retroviral transduction with shRNA/Kusabira-Orange (KO) expressors. Leukemic cells highly expressing KO were sorted and immediately transplanted into secondary recipient mice. (B) Relative-relative expression levels of *Bahcc1* in shRNA-transduced leukemic cells. shLuc, shRNA against *luciferase*; shB-2, shRNA against *Bahcc1*. (C) Survival curves of mice transplanted with *Bahcc1*-depleted (shB-2; n = 12) or control (shLuc; n = 10) leukemic cells. Data from 3 independent experiments were combined. (D) Spleen weights of moribund mice. (E) Representative FACS plots of BM cells from moribund mice. GFP/KO doubly positive cells were gated as shown in the top panels, followed by subsequent analyses for c-kit, Gr-1, and CD11b expression. (F) Relative-relative expression levels of *Bahcc1* by RT-qPCR in BM cells from moribund mice. Bar graphs show the mean with SD of at least 3 independent experiments. ns, not significant (log-rank test for panel C and unpaired Welch *t* tests for panels D-E). Wt, wild-type.

although knock-in mice harboring the mutation abrogating BAH function did not exhibit alterations in hematopoiesis.[23]

In conclusion, LT-HSCs among HSPCs showed greatest susceptibility to *MLL-ENL*–mediated immortalization. In an analysis of immortalization potential, Bahcc1 was found to be a key molecule. MLL-ENL upregulated *Bahcc1*, and *Bahcc1* depletion suppressed *MLL-ENL*–mediated leukemogenesis in vivo and in vitro, at least partly through derepression of H3K27me3-marked *Cdkn1c*. Taken together, these results demonstrate an important role of the *MLL-fusion-Bahcc1* axis that may lead to applications in molecular targeted therapy.

Acknowledgments

The authors thank Toshio Kitamura (The Institute of Medical Science, University of Tokyo) for providing pMXsU6-puro and THP-1 cells, Akihiko Yokoyama (Tsuruoka Metabolomics Laboratory, National Cancer Center) for providing HB1119 cells, Japan Medical Communication (Fukuoka, Japan) and PALABRA Inc. (Kyoto, Japan) for language assistance, and Rukia Iwayama for technical support.

This work was supported in part by grants-in-aid from the Ministry of Education, Culture, Sports, Science, and Technology in Japan (TN; Basic-B 17H04227, RO; Basic-C 21K08411).

The funders had no role in study design, data collection and interpretation, or the decision to submit the work for publication.

Authorship

Contribution: A.N., T.N., and R.O. designed the study, analyzed the data, interpreted the results, and wrote the manuscript; A.N., M.M., M.S., and R.O. performed in vitro experiments; A.N., I.T., and R.O. performed in vivo experiments; and I.T., T.N., and R.O. contributed to study supervision.

Conflict-of-interest disclosure: The authors declare no competing financial interests.

ORCID profiles: I.T., 0000-0002-5426-9422; T.N., 0000-0002-0037-7049.

Correspondence: Ryoichi Ono, Department of Microbiology and Molecular Genetics, Mie University Graduate School of Medicine, 2-174 Edobashi, Tsu, Mie 514-8507, Japan; email: rono-mie@doc.medic.mie-u.ac.jp.

References

1. Bonnet D, Dick JE. Human acute myeloid leukemia is organized as a hierarchy that originates from a primitive hematopoietic cell. *Nat Med*. 1997;3(7):730-737.
2. Passegué E, Jamieson CHM, Ailles LE, Weissman IL. Normal and leukemic hematopoiesis: Are leukemias a stem cell disorder or a reacquisition of stem cell characteristics? *Proc Natl Acad Sci U S A*. 2003;100(suppl 1):11842-11849.
3. Carroll D, St Clair DK. Hematopoietic stem cells: normal versus malignant. *Antioxid Redox Signal*. 2018;29(16):1612-1632.
4. Velten L, Story BA, Hernandez-Malmierca P, et al. Identification of leukemic and pre-leukemic stem cells by clonal tracking from single-cell transcriptomics. *Nat Commun*. 2021;12(1):1366.
5. Chen W, Kumar AR, Hudson WA, et al. Malignant transformation initiated by Mll-AF9: gene dosage and critical target cells. *Cancer Cell*. 2008;13(5):432-440.
6. Shlush LI, Zandi S, Mitchell A, Chen WC, Brandwein JM, Gupta V, Kennedy JA, Schimmer AD, Schuh AC, Yee KW, McLeod JL, Doedens M, Medeiros JJF, Marke R, Kim HJ, Lee K, McPherson JD, Hudson TJ, HALT Pan-Leukemia Gene Panel Consortium, Brown AMK, Yousif F, Trinh QM, Stein LD, Minden MD, Wang JCY, Dick JE. Identification of pre-leukaemic haematopoietic stem cells in acute leukaemia. *Nature*. 2014;506(7488):328-333.
7. Stavropoulou V, Kaspar S, Brault L, et al. MLL-AF9 expression in hematopoietic stem cells drives a highly invasive AML expressing EMT-related genes linked to poor outcome. *Cancer Cell*. 2016;30(1):43-58.
8. Chen X, Burkhardt DB, Hartman AA, et al. MLL-AF9 initiates transformation from fast-proliferating myeloid progenitors. *Nat Commun*. 2019;10(1):5767.
9. Ono R, Masuya M, Nakajima H, et al. Plzf drives MLL-fusion-mediated leukemogenesis specifically in long-term hematopoietic stem cells. *Blood*. 2013;122(7):1271-1283.
10. Kiel MJ, Yilmaz OH, Iwashita T, Yilmaz OH, Terhorst C, Morrison SJ. SLAM family receptors distinguish hematopoietic stem and progenitor cells and reveal endothelial niches for stem cells. *Cell*. 2005;121(7):1109-1121.
11. Morita Y, Ema H, Nakauchi H. Heterogeneity and hierarchy within the most primitive hematopoietic stem cell compartment. *J Exp Med*. 2010;207(6):1173-1182.
12. Boles NC, Lin KK, Lukov GL, Bowman TV, Baldridge MT, Goodell MA. CD48 on hematopoietic progenitors regulates stem cells and suppresses tumor formation. *Blood*. 2011;118(1):80-87.
13. Pietras EM, Reynaud D, Kang YA, et al. Functionally distinct subsets of lineage-biased multipotent progenitors control blood production in normal and regenerative conditions. *Cell Stem Cell*. 2015;17(1):35-46.
14. Chen J, Odenike O, Rowley JD. Leukemogenesis: more than mutant genes. *Nat Rev Cancer*. 2010;10(1):23-36.
15. Bernt KM, Zhu N, Sinha AU, et al. MLL-rearranged leukemia is dependent on aberrant H3K79 methylation by DOT1L. *Cancer Cell*. 2011;20(1):66-78.
16. Greenblatt SM, Nimer SD. Chromatin modifiers and the promise of epigenetic therapy in acute leukemia. *Leukemia*. 2014;28(7):1396-1406.

17. Kitamura T, Watanabe-Okochi N, Enomoto Y, et al. Novel working hypothesis for pathogenesis of hematological malignancies: combination of mutations-induced cellular phenotypes determines the disease (cMIP-DD). *J Biochem*. 2016;159(1):17-25.
18. Dawson MA. The cancer epigenome: concepts, challenges, and therapeutic opportunities. *Science*. 2017;355(6330):1147-1152.
19. Ernst T, Chase AJ, Score J, et al. Inactivating mutations of the histone methyltransferase gene EZH2 in myeloid disorders. *Nat Genet*. 2010;42(8):722-726.
20. Nikoloski G, Langemeijer SM, Kuiper RP, et al. Somatic mutations of the histone methyltransferase gene EZH2 in myelodysplastic syndromes. *Nat Genet*. 2010;42(8):665-667.
21. Morin RD, Johnson NA, Severson TM, et al. Somatic mutations altering EZH2 (Tyr641) in follicular and diffuse large B-cell lymphomas of germinal-center origin. *Nat Genet*. 2010;42(2):181-185.
22. Blackledge NP, Klose RJ. The molecular principles of gene regulation by Polycomb repressive complexes. *Nat Rev Mol Cell Biol*. 2021;22(12):815-833.
23. Fan H, Lu J, Guo Y, et al. BAHCC1 binds H3K27me3 via a conserved BAH module to mediate gene silencing and oncogenesis. *Nat Genet*. 2020;52(12):1384-1396.
24. Fan H, Guo Y, Tsai YH, et al. A conserved BAH module within mammalian BAHD1 connects H3K27me3 to Polycomb gene silencing. *Nucleic Acids Res*. 2021;49(8):4441-4455.
25. Gough SM, Lee F, Yang F, et al. NUP98-PHF23 is a chromatin-modifying oncoprotein that causes a wide array of leukemias sensitive to inhibition of PHD histone reader function. *Cancer Discov*. 2014;4(5):564-577.
26. Ono R, Masuya M, Inoue N, et al. Tet1 is not required for myeloid leukemogenesis by MLL-ENL in novel mouse models. *PLoS One*. 2021;16(3):e0248425.
27. Kitamura T, Koshino Y, Shibata F, et al. Retrovirus-mediated gene transfer and expression cloning: powerful tools in functional genomics. *Exp Hematol*. 2003;31(11):1007-1014.
28. Ono R, Kumagai H, Nakajima H, et al. Mixed-lineage-leukemia (MLL) fusion protein collaborates with Ras to induce acute leukemia through aberrant Hox expression and Raf activation. *Leukemia*. 2009;23(12):2197-2209.
29. Ono R, Masuya M, Ishii S, Katayama N, Nosaka T. Eya2, a target activated by Plzf, is critical for PLZF-RARA-induced leukemogenesis. *Mol Cell Biol*. 2017;37(13):e00585-16-16.
30. Ono R, Nakajima H, Ozaki K, et al. Dimerization of MLL fusion proteins and FLT3 activation synergize to induce multiple-lineage leukemogenesis. *J Clin Invest*. 2005;115(4):919-929.
31. Wang Y, Krivtsov AV, Sinha AU, et al. The Wnt/beta-catenin pathway is required for the development of leukemia stem cells in AML. *Science*. 2010;327(5973):1650-1653.
32. Goveas N, Waskow C, Arndt K, et al. MLL1 is required for maintenance of intestinal stem cells. *PLoS Genet*. 2021;17(12):e1009250.
33. Miyamoto R, Kanai A, Okuda H, et al. HOXA9 promotes MYC-mediated leukemogenesis by maintaining gene expression for multiple anti-apoptotic pathways. *eLife*. 2021;10:e64148.
34. Prange KHM, Mandoli A, Kuznetsova T, et al. MLL-AF9 and MLL-AF4 oncofusion proteins bind a distinct enhancer repertoire and target the RUNX1 program in 11q23 acute myeloid leukemia. *Oncogene*. 2017;36(23):3346-3356.
35. Ito J, Yamagata K, Shinohara H, et al. Dual inhibition of EZH1/2 induces cell cycle arrest of B cell acute lymphoblastic leukemia cells through upregulation of CDKN1C and TP53INP1. *Int J Hematol*. 2023;117(1):78-89.
36. Balgobind BV, Van den Heuvel-Eibrink MM, De Menezes RX, et al. Evaluation of gene expression signatures predictive of cytogenetic and molecular subtypes of pediatric acute myeloid leukemia. *Haematologica*. 2011;96(2):221-230.
37. Metzelder SK, Michel C, von Bonin M, et al. NFATc1 as a therapeutic target in FLT3-ITD-positive AML. *Leukemia*. 2015;29(7):1470-1477.
38. Bild AH, Yao G, Chang JT, et al. Oncogenic pathway signatures in human cancers as a guide to targeted therapies. *Nature*. 2006;439(7074):353-357.
39. Pigazzi M, Masetti R, Bresolin S, et al. MLL partner genes drive distinct gene expression profiles and genomic alterations in pediatric acute myeloid leukemia: an AIEOP study. *Leukemia*. 2011;25(3):560-563.
40. Stavropoulou V, Almosailleakh M, Royo H, et al. A novel inducible mouse model of MLL-ENL-driven mixed-lineage acute leukemia. *Hemasphere*. 2018;2(4):e51.
41. Ugale A, Norddahl GL, Wahlestedt M, et al. Hematopoietic stem cells are intrinsically protected against MLL-ENL-mediated transformation. *Cell Rep*. 2014;9(4):1246-1255.
42. Milne TA. Mouse models of MLL leukemia: recapitulating the human disease. *Blood*. 2017;129(16):2217-2223.
43. Almosailleakh M, Schwaller J. Murine models of acute myeloid leukaemia. *Int J Mol Sci*. 2019;20(2):453.
44. Matsuoka S, Edwards MC, Bai C, et al. p57KIP2, a structurally distinct member of the p21CIP1 Cdk inhibitor family, is a candidate tumor suppressor gene. *Genes Dev*. 1995;9(6):650-662.
45. Zhou K, Zhou M, Cheng L, et al. Loss of MBD2 attenuates MLL-AF9-driven leukemogenesis by suppressing the leukemic cell cycle via CDKN1C. *Oncogene*. 2021;10(11):79.
46. Bill M, Mrózek K, Kohlschmidt J, et al. Mutational landscape and clinical outcome of patients with de novo acute myeloid leukemia and rearrangements involving 11q23/KMT2A. *Proc Natl Acad Sci U S A*. 2020;117(42):26340-26346.